Stereotactic and Functional Neurosurgery

Manuscript:	SFN-2023-9-6/R1 RESUBMISSION
Title:	Evaluation of 3D C-arm fluoroscopy versus diagnostic CT for Deep Brain Stimulation stereotactic registration and post-operative lead localisation
Authors(s):	James Manfield (Corresponding Author), Sean Martin (Co-author), Alexander Laurence Green (Co-author), James FitzGerald (Co-author)
Keywords:	Deep brain stimulation, Functional neurosurgery, Image-guided neurosurgery, Movement disorder surgery, Movement disorders, Stereotactic surgery
Type:	Research Article

Oxford University Hospitals NHS
NHS Trust

Oxford Functional Neurosurgery

01 December 2023

Dear Dr Lozano,

Re: Manuscript: SFN-2023-9-6 - Evaluation of 3D C-arm fluoroscopy versus diagnostic CT for Deep Brain Stimulation stereotactic registration and post-operative lead localisation

We greatly thank the reviewers for their comments and the editor for the opportunity to revise the manuscript to address them.

Below we provide a point by point description of the changes we have made in response to each comment.

Reviewer 1:

The authors report on technical accuracy of electrode placement in DBS, comparing different imaging modalities, including recently introduced 3D mobile devices. They highlight the of x-ray based 3D imaging to receive distortion free and accurate coordinates of the electrode tip position. The use of 3d fluoroscopes and other mobile devices are proven to have no disadvantages but should be included in the routine setting for planning, intraoperative control and postoperative confirmation.
Although there is just a limited impact for patients clinical outcome, the study is important for keeping DBS setting more flexible without losing (but improving) accuracy. I therefore recommend publication of this well written manuscript.

We thank the reviewer for their comments

Reviewer 2:

Comments to authors
In the present manuscript, Fitzgerald and colleagues critically assess the capabilities of 3D C-arm fluoroscopy (3DXT) as an alternative to conventional CT, especially given the cost and bulk associated with portable imaging technologies such as the Medtronic O-arm® and mobile CT. Using a sample of 15 patients, with a total of 29 leads, the authors present a comparison of 3DXT and CT fusion with pre-operative MRI. The results underscore the marginally (and surprising) superior registration accuracy of 3DXT over CT, coupled with its significantly reduced radiation exposure (~20%). Despite certain limitations inherent to 3DXT, this study makes a compelling argument for its potential as a cost-effective, viable substitute for CT, particularly in resource-constrained settings.

Again we thank the reviewer for their constructive comments

Typos and Grammar:
On Line 110, the phrase "Registration must there be performed..." should be corrected to "Registration must

therefore be performed..."
In Line 308, the term “simulation” should be replaced with “stimulation”.

We have duly corrected these in their corresponding lines

Methodological Concerns:
A crucial aspect that needs elaboration is the specific methodology employed to calculate the Euclidean and radial distances. The current description leaves the reader pondering whether these calculations were conducted manually using post-operative radiographic software or automated through a dedicated code-based algorithms. If manual measurements were undertaken, details such as the number of measurements and the number of users involved would provide invaluable context. A more comprehensive explanation on this front would greatly enhance the manuscript's clarity.

We are grateful to the reviewer for this helpful suggestion to improve the manuscript’s clarity. Both the fusion and targeting accuracy measurements were undertaken manually and all by the same author (JM) to ensure methodological consistency and minimise unwanted variation. One measurement was taken per scan at target (for targeting accuracy assessment) and electrode tip (for fusion assessment). We have added further methodological elaboration in lines 192 to 193 here.

Yours Sincerely,

Dr James Manfield FRCS (on behalf of co-authors)

Department of Neurological Surgery, The John Radcliffe Hospital, Headley Way, Oxford, OX3 9DU

Evaluation of 3D C-arm fluoroscopy versus diagnostic CT for Deep Brain Stimulation stereotactic registration and post-operative lead localisation

Running Title: 3D fluoroscopy versus CT for DBS registration and lead localisation

James Manfield[1*]
Sean Martin[1]
Alexander L Green[1 2]
James J Fitzgerald [1 2]

[1]Oxford Functional Neurosurgery, John Radcliffe Hospital, Headley Way, Headington, Oxford, OX3 9DU UK
[2]Nuffield Department of Surgical Sciences, University of Oxford, Oxford, UK

*Denotes corresponding author jmanfield@nhs.net

Keywords: DBS imaging; 3D fluoroscopy; robot assisted DBS

Abstract

Introduction

DBS efficacy depends on accuracy. CT-MRI fusion is established for both stereotactic registration and electrode placement verification. The desire to streamline DBS workflows, reduce operative time and minimize patient transfers has increased interest in portable imaging modalities such as the Medtronic O-arm® and mobile CT. However, these remain expensive and bulky. 3D C-arm fluoroscopy (3DXT) units are a smaller and less costly alternative, albeit incompatible with traditional frame-based localisation and without useful soft tissue resolution.

We aimed to compare fusion of 3DXT and CT with pre-operative MRI to evaluate if 3DXT-MRI fusion alone is sufficient for accurate registration and reliable targeting verification. We further assess DBS targeting accuracy using a 3DXT workflow and compare radiation dosimetry between modalities.

Methods

Patients underwent robot-assisted DBS implantation using a workflow incorporating 3DXT which we describe. Two intra-operative 3DXT spins were performed for registration and accuracy verification followed by conventional CT post-operatively.

Post-operative 3DXT and CT images were independently fused to the same pre-operative MRI sequence and co-ordinates generated for comparison.

Registration accuracy was compared to 15 consecutive controls who underwent CT based registration. Radial targeting accuracy was calculated, and radiation dosimetry recorded.

Results

Data were obtained from 29 leads in 15 consecutive patients. 3DXT registration accuracy was significantly superior to CT with mean error 0.22 ±0.03mm ($p<0.0001$).

Mean Euclidean electrode tip position variation for CT to MRI versus 3DXT to MRI fusion was 0.62 ±0.40mm (range 0.0mm – 1.7mm). In comparison, direct CT to 3DXT fusion showed electrode tip Euclidean variance of 0.23 ±0.09mm.

Mean radial targeting accuracy assessed on 3DXT was 0.97 ±0.54mm vs 1.15 ± 0.55mm on CT with differences insignificant ($p = 0.30$).

Mean patient radiation doses were around 80% lower with 3DXT vs CT ($p<0.0001$).

Discussion

Mobile 3D C-arm fluoroscopy can be safely incorporated into DBS workflows for both registration and lead verification. For registration, the limited field of view requires the use of frameless transient fiducials and is highly accurate. For lead position verification based on MRI co-registration, we estimate there is around a 0.4mm discrepancy between lead position seen on 3DXT vs CT when corrected for brain-shift. This is similar to that described in O-arm® or mobile CT series. For units where logistical or financial considerations preclude the acquisition of a cone beam CT or mobile CT scanner, our data support portable 3D C-arm fluoroscopy as an acceptable alternative with significantly lower radiation exposure.

Introduction

DBS efficacy relies on accurate lead targeting[1]. Whilst stereotactic MRI has been regarded by some as the gold standard imaging modality[2], CT-MRI co-registration is an established method for both stereotactic registration and lead placement verification[3]. Fusion inevitably introduces some error, but numerous studies have now quantified this as acceptably small for clinical use[4]. Mobile CT scanners are costly and not yet widely available, so whilst far quicker than MRI, obtaining a CT still typically entails a trip from the operating room. This needs to be repeated twice if used for both stereotactic registration and target confirmation. The desire to streamline DBS workflows, reduce operative time and minimize patient transfers has led to increasing interest in mobile imaging modalities. There are now several published reports using the O-arm® (Medtronic Inc.; Minneapolis, USA), a portable cone beam CT (CBCT) device utilised extensively for spinal surgery, establishing it as a viable option for both DBS stereotactic registration and lead position confirmation[5, 6, 4]. The drawbacks of O-arm include its large footprint, which is not compatible with all operating room set-ups, and expense[7]. We have accordingly acquired the smallest second-generation 3D fluoroscopic C-arm (3DXT; Ziehm RFD 3D, Ziehm Imaging, Germany), which is approximately half the current cost of an O-arm and a similar size to a conventional 2D C-arm. The RFD 3D generates the same power as

an O-arm II with a smaller pixel size, giving the two devices similar bony imaging quality. Among the new 3D-fluoroscopy units, the RFD 3D offers the widest compatibility and integrates with most navigation and robotics platforms[7] – including our recently introduced robot-assisted stereotactic DBS workflow. It does however lack the enhanced soft tissue imaging mode of the O-arm, meaning intra-cranial soft tissue delineation is negligible (See Figure 1). Furthermore, the 20cm field of view (effectively half that of the O-arm's) means an entire human cranium cannot typically be captured within the elliptical 3D spin field and precludes conventional frame based stereotactic registration. Registration must therefore be performed via frameless transient fiducials (FTFR), for which accuracy is established[8]. In view of these limitations of 3DXT, and the lack of published reports supporting its use in DBS, we have further obtained at 24 hours post-op a diagnostic CT scan for confirmation of electrode position, exclusion of significant haematoma prior to discharge, and reconstruction of directional lead contacts[9].

We aim to compare fusion of 3DXT and diagnostic CT with pre-operative planning MRI to evaluate if MRI fusion with 3DXT alone is sufficient for both accurate registration and reliable targeting verification. We further assess DBS targeting accuracy using the 3DXT based workflow, and compare radiation dosimetry between the two modalities.

FIGURE 1 (Comparison of Ziehm RFD 3D and Medtronic O-arm II imaging Appearances)

A. Post-operative DBS Ziehm RFD 3D example imaging- the absence of soft tissue resolution is apparent. B Medtronic O-arm II (3D enhanced mode) example post-DBS image. Here, the rudimentary soft tissue delineation can be appreciated – sufficient for instance to show ventricular configuration.

Figure B image courtesy of Medtronic Inc., reproduced with permission.

Methods

DBS Surgical workflow

Patients underwent robot-assisted DBS implantation using an adapted workflow to incorporating 3DXT in lieu of CT. All patients underwent pre-operative 3T MRI sequences on which the surgical

targeting plan was performed. The Parkinson's disease and dystonia cases were all performed under general anaesthesia with direct targeting. Tremor cases utilising VIM as the surgical target were performed under local anaesthesia +/- conscious sedation to enable intra-operative macrostimulation and assessment. In all cases the CRW frame base ring was used as a head-holder attached to a stereotactic robot (Neuromate; Renishaw, UK). Frameless transient fiducial registration was performed in theatre with a geometrical array mounted on the robotic arm (Neurolocate; Renishaw, UK) in conjunction with a mobile 3DXT (RFD 3D, Ziehm Imaging, Germany). Initial AP and lateral 2D radiographs were obtained to confirm alignment and field of view followed by a 3D spin (Settings: Matrix size 512 x 512, slice thickness – 0.39mm, number of slices 512.) The images were exported to the robotic planning station and detected fiducials manually adjusted until a registration accuracy of <0.25mm was obtained. Image fusion was performed between 3DXT and pre-operative MRI and manually checked. In all cases a fine cut 3D T1-weighted gradient echo was used as the base sequence. A test trajectory to a staple placed on the patient's head prior to imaging was also performed to verify accuracy. The DBS leads were then inserted in keeping with previously described robotic assisted surgical techniques e.g. [10]. Following electrode insertion, a second 3DXT scan was obtained and again fused with pre-operative imaging to confirm targeting accuracy. Following assessment as satisfactory, the case was completed via implantable pulse generator insertion and definitive closure of all wounds. All patients underwent a diagnostic CT scan at 24 hours post op using the same CT scanner in all cases (Siemens Naeotom Alpha, Siemens, Germany) employing a standard CT brain protocol with the following parameters: Acquisition 96 x 0.4mm Volume CT dose index: 55.7; Pitch: 0.35; Rotation Time(s) 0.5; Reconstruction Slice Thickness: 0.6mm; Slice Increment: 0.4mm; Reconstruction Kernel: HR44; Quantum Iterative Reconstruction (QIR) strength: 3; Matrix size: 512 x 512).

FIGURE 2 (DBS Workflow Summary)

Data assessment and analysis

The post-operative 3DXT and diagnostic CT scans were both independently fused to the same pre-operative 3T T1 weighted MR sequence, on which AC-PC co-ordinates had been defined. A trajectory target point was independently created at the tip of the distal electrode contact visualised on CT and 3DXT respectively and co-ordinates generated. To minimise any confounding variation, the right sided contact was always used in bilateral procedures, unless this electrode had been moved

following the 3DXT check scan, in which case the left sided lead was employed. Consistent sequences with equivalent slice thickness (0.4mm for CT and 0.39mm for 3DXT) and standardised windowing settings were employed in all cases. These were chosen so that the tip of the distal contact was unambiguous on multiplanar imaging. The electrode tip was selected as a clear and readily reproducible landmark.

To quantify the impact of post-operative brain shift (e.g. following resolution of any pneumocephalus) rather than fusion variance per se resulting in electrode position discrepancy, the 3DXT and CTs scans were also fused directly to each other as well and co-ordinates generated in the same fashion.

The Euclidean (comprising x, y and z variation) and radial (comprising x and y only) variance between the two generated co-ordinates was calculated using standard formulae[11, 3]. The Euclidean distance is the square root of the sum of squares of the differences in the x, y, and z directions i.e. $\sqrt{[(\Delta x)^2 + (\Delta y)^2 + (\Delta z)^2]}$ with radial comprising $\sqrt{[(\Delta x)^2 + (\Delta y)^2]}$. Vector components were also considered individually.

Registration accuracy is automatically calculated by the planning software based on comparison of the detected to expected fiducial positions. For comparative purposes, data were also obtained from 15 consecutive control cases who underwent conventional CT based registration with CRW frame localiser fiducial box. These cases were performed immediately prior to the introduction for 3DXT and FTFRs and so temporally adjacent. The same planning software was employed in all cases (Renishaw, UK).

Radial targeting accuracy was calculated based on the measured distance between the observed and planned target (typically set at the middle of the first directional contact) as opposed to the electrode tip. All fusion and targeting accuracy assessments were performed manually by the same author to further ensure methodological consistency and minimise variation.

Finally, radiation dosimetry from both scans were noted from contemporaneous documentation.

Results

Patient characteristics

Data were obtained from 29 leads in 15 consecutive patients. All but 1 underwent bilateral DBS insertion involving intra-operative 3DXT and post-operative CT. Patient details are summarised in Table 1.

TABLE 1 (3DXT Patient Characteristics)

Registration Accuracy

For registration with 3DXT plus frameless transient fiducials (FTR), mean registration error was 0.22 ±0.03 mm. For the 15 patient control group with CRW fiducial localiser box CT-based registration, mean error was 0.35 ±0.05 mm. Differences were statistically significant (t test $p<0.0001$) favouring 3DXT.

Demographics between the two groups were very similar with the CT control group having the same sex mix (male:female 6:9) and mean age 63 ± 8.1.

Fusion Variation Assessment

Mean electrode tip position Euclidean variation measured between CT to MRI and 3DXT to MRI fusion was 0.62 ±0.40 mm with range 0.0mm – 1.7mm. Mean radial fusion variance was 0.41mm ± 0.26 mm with range 0.0 mm – 1.1mm.

Mean absolute variation in tip co-ordinates as assessed on 3DXT vs CT to MRI fusion were x 0.22mm (range 0-0.6mm), y 0.28mm (range 0-0.9mm) and z 0.4mm (range 0-1.3mm)

In comparison, direct CT to 3DXT fusion showed electrode tip Euclidean variance of 0.23 ±0.09 mm and radial variance of 0.18mm ±0.08 mm.

Vector components:

Compared with CT-MRI fusion, tip co-ordinates as assessed via 3DXT-MRI fusion were a mean (range) of:

0.007 mm (-0.6 to + 0.4) **right**

0.15 mm (-1 to + 0.4) **posterior**

0.06 mm (-0.9 to +1.3) **superior**

FIGURE 3 (Comparison of electrode tip position as assessed on CT-MRI vs 3DXT-MRI fusions)

Figure A shows an axial 3DXT image fused to 3T MRI FLAIR with crosshair placed over middle of electrode tip position. In Figure B, the CT is fused with the same MRI sequence. The crosshair is unmoved and electrode position can be seen to appear more lateral (c. 0.5mm which approximates to the 0.41mm average radial fusion variation seen in this series).

Figure C (3DXT to MRI FLAIR fusion) and Figure D (CT to MRI FLAIR fusion) demonstrate the same again, but here the discrepancy is more marked with the electrode on CT appearing anterior and lateral to its position on 3DXT with radial variation c. 1.1mm (the maximum observed in this series).

Targeting Accuracy Assessment

Absolute X and Y deviation at planned target as measured on CT-MRI fusion were x mean 0.62mm (SD 0.62mm, range 0-1.47mm) and y 0.31mm (SD 0.54mm, range 0.15-2.1mm). Mean radial error was 1.15mm (SD 0.55mm range 0.3-2.12mm).

Assessed on 3DXT-MRI fusion, absolute x and y deviation were x mean 0.66mm (SD 0.38mm, range 0 -1.24mm) and y mean 0.63mm (SD 0.50mm range 0-1.77mm). Mean radial error was 0.97mm (SD 0.54mm, range 0.26-2.14mm). Assessment differences between the two modalities were not significant (t-test p =0.30).

TABLE 2 (Targeting Accuracy Comparison)

Radiation Dosimetry

Mean CT radiation dose was 942(±54) mGycm. Data were normally distributed (Shapiro-Wilk P = 0.15). This equates to an approximate effective dose of 1.89 mSv [12, 13].

Mean 3DXT radiation doses was 270.1(±74.3) cGycm^2, with all patients receiving two 3D spins. Data were also normally distributed (P = 0.50). Mean approximate absorbed dose was 0.35 mSv (SD 0.10, range 0.21-0.50 mSv). These were significantly less than CT absorbed doses (t test p<0.0001).

Discussion

We have evaluated intra-operative 3DXT use via a 3D C-arm for 29 DBS lead insertions in 15 patients. The mean registration error with 3DXT plus FTFR of 0.22 ±0.03 mm represented a significant improvement compared to our prior CT and frame-based technique. The absolute improvement value of mean 0.13mm is of doubtful clinical significance in isolation but of course contributes to the cumulative error.

Regarding electrode tip localisation, there was a 0.62 ±0.40 mm discrepancy between CT and 3DXT MRI fusion assessment. Part of this variance can be explained by the 24-hour time interval between the scans with re-accumulation of CSF etc. We estimate this effect to explain an average variance of 0.23 ±0.09 mm based on fusing the 3DXT to CT modalities together directly. Such a bone to bone 3DXT to CT fusion has been shown to be highly accurate[14] with minimal error. This leaves a net residual variation of under 0.4mm which may fall within the limitations of human measurement error - other authors for instance have estimated this effect to be around 0.62- 0.7mm[5, 6].

The results should be interpreted in the context that CT to MRI fusion, whilst widely established, remains an intrinsically imperfect process and indeed identical CT and MRI image pairs can produce differing electrode locations, with a median variance of 0.57mm (0.49-0.76mm) noted in one recent study[15], depending on the particular co-registration approach utilised. The software platform used here has been suggested to be amongst the most accurate CT/MRI co-registration algorithms[16] and found to have a geometric fusion error of 0.72 ± 0.08mm[16]. Evaluation of image co-registration typically assumes there is a single ideal solution where the two scans are effectively identical. This may not be entirely true, for instance application of the stereotactic frame adds artifact and distorts scalp outline in addition to the potential geometric distortion of MRI data -particularly with increasing field strength.

These results are comparable to studies evaluating CBCT e.g. O-arm vs CT to MRI co-registration which have for instance found a mean Euclidean difference of 0.886 ±0.190 mm[4]. The interpretation that C-arm based 3DXT is an acceptable alternative to CBCT or CT based techniques is also supported by our overall targeting accuracy results, as assessed on postoperative CT. These subsume both the 3DXT registration scan and the 3DXT post operative check scan on review of

which the decision to accept the final lead position was made. In line with other authors' approach e.g.[17], we have assessed radial accuracy only here as we have found most depth (z coordinate) inaccuracies to be attributable to operator electrode fixation, and easily remediable following the intra-op check scan. The post operative CT imaging therefore reflects any z corrections made following the 3DXT check scan. Radial accuracy is furthermore the most clinically relevant measurement as it directly impacts stimulation efficacy and unwanted effects. Our CT assessed radial accuracy of 1.15 ±0.55 mm was not significantly different from the 0.97 ±0.54 mm as measured on the intra-op 3DXT check scan, and compares acceptably to other published DBS accuracy results[18]. There were no cases where the difference in apparent lead position between the 3DXT and subsequent CT was sufficient to warrant electrode revision.

On a practical note, the 20cm 3DXT 3D FOV means that some of the cranium is typically truncated for the 3D spin. It is suggested that as much of the skull base as possible should be included for an optimum fusion[4]. The outlier case in this series demonstrated a Euclidean fusion discrepancy of 1.7mm (and radial 1.1mm- see Figure 1). We speculate this was caused by mild movement artifact on the MRI scan leading to some peripheral image distortion. With no soft tissue resolution, the 3DXT to MRI fusion relies on fewer data (entirely bony anatomy) and it is thus plausible that it would be subject to greater influence by such image distortion.

Post-operative MRI has its own well known limitations including the size of the electrode related signal void meaning for instance a 1.3mm DBS electrode typically appears to be 2-4mm in diameter[1, 16]. Thus, regardless of the imaging modality employed, some uncertainty surrounding the exact lead position at present remains. Furthermore, due to the aforementioned limited field of view, it is not possible to perform stereotactic imaging with 3DXT. Without stereotactic imaging to generate independent co-ordinates, we cannot conclude from these data which fusion approach (3DXT vs CT) most accurately represents the true position of the electrode. Our conclusions are thus limited to quantifying the variation between the modalities, but support the premise that 3DXT is an acceptable CT or CBCT alternative. There may however be scope for further improvement in 3DXT-MRI fusion. For instance one recent study evaluating a mobile CT scanner (Brainlab Airo) found only a 0.36(±0.54)mm fusion variation between that and conventional CT[19]. Other authors have also described modified 3DXT workflows with for example the addition of IV contrast and region of interest fusion to improve fusion accuracy[20]. Future studies should attempt to quantify the impact of such additional measures to improve 3DXT-MRI fusion accuracy.

Mean patient radiation dose from the two 3DXT spins comprised around 19% of our diagnostic CT doses, and compare favourably to CBCT doses reported in the literature which are typically between 50-100% of conventional CT imaging doses[6, 7, 4]. However, a direct comparison of patient

radiation exposures delivered by CT or CBCT and 3DXT is not possible, as dosimetry is expressed in dose-area product (DAP; mGy.cm.) for 3DXT. and in dose-length product (DLP; mGy.cm) for CBCT and CT. Application of the effective dose (ED) as employed here facilitates estimated comparison of radiation doses from differing modalities by applying appropriate conversion factors to DLP or DAP[21, 22].

Conclusions

Mobile 3D C-arm fluoroscopy can be safely incorporated into DBS workflows for both registration and lead verification purposes. For registration, the limited field of view requires the use of frameless transient fiducials and is highly accurate. For lead position verification based on MRI co-registration, we estimate there is around a net 0.4mm discrepancy between lead position seen on 3DXT vs diagnostic CT when corrected for brain-shift. This is a similar order of magnitude to that described with the well-studied O-arm® and mobile CT scanners. Effective radiation doses for two 3DXT spins were around 20% of conventional CT. For neurosurgical units where logistical or financial considerations preclude the acquisition of a cone beam CT or mobile CT scanner, our data support portable 3D C-arm fluoroscopy as an acceptable alternative.

Statement of Ethics

The study is a service evaluation via retrospective case series review containing no identifiable patient data, for which formal ethical approval was not required (see http://www.hra-decisiontools.org.uk/ethics/ which contains an algorithm to determine what studies require ethical approval in the UK). The 3D C-arm utilised is an approved CE-marked medical device which has neither been modified nor is being used outside of its intended purpose. All patients supplied written informed consent to undergo robot-assisted DBS surgery comprising 3DXT intra-operative and post-operative imaging and for the use of anonymised data for study participation.

Conflict of Interest Statement

The authors have no conflicts of interest to declare.

Funding Sources

This study was not supported by any sponsor or funder.

Author Contributions

JM co-conceived the study, collected data and drafted the manuscript. SM collected data and co-edited the manuscript. JM and JJF analysed data with important intellectual input from AG. All authors critically revised the manuscript.

Data Availability Statement

The data that support the findings of this study are not publicly available due to patient confidentiality but are available from the corresponding author [JM] [jmanfield@nhs.net] subject to necessary anonymisation upon reasonable request.

References

1. Mirzadeh Z, Chapple K, Lambert M, Dhall R, Ponce FA. Validation of CT-MRI fusion for intraoperative assessment of stereotactic accuracy in DBS surgery. Movement Disorders. 2014;29(14):1788-95.
2. Bot M, Van Den Munckhof P, Bakay R, Stebbins G, Verhagen Metman L. Accuracy of intraoperative computed tomography during deep brain stimulation procedures: comparison with postoperative magnetic resonance imaging. Stereotactic and Functional Neurosurgery. 2017;95(3):183-88.
3. Furlanetti L, Hasegawa H, Oviedova A, Raslan A, Samuel M, Selway R, et al. O-arm stereotactic imaging in deep brain stimulation surgery workflow: a utility and cost-effectiveness analysis. Stereotactic and Functional Neurosurgery. 2021;99(2):93-106.
4. Peng T, Kramer DR, Lee MB, Barbaro MF, Ding L, Liu CY, et al. Comparison of intraoperative 3-dimensional fluoroscopy with standard computed tomography for stereotactic frame registration. Operative Neurosurgery. 2020;18(6):698.
5. Holloway K, Docef A. A quantitative assessment of the accuracy and reliability of O-arm images for deep brain stimulation surgery. Operative Neurosurgery. 2013;72:ons 47-ons 57.
6. Carlson JD, McLeod KE, McLeod PS, Mark JB. Stereotactic accuracy and surgical utility of the O-arm in deep brain stimulation surgery. Operative Neurosurgery. 2017;13(1):96-107.
7. Malham GM, Wells-Quinn T. What should my hospital buy next?—guidelines for the acquisition and application of imaging, navigation, and robotics for spine surgery. Journal of Spine Surgery. 2019;5(1):155.

8. Hines K, Matias CM, Leibold A, Sharan A, Wu C. Accuracy and efficiency using frameless transient fiducial registration in stereoelectroencephalography and deep brain stimulation. Journal of Neurosurgery. 2022;1(aop):1-7.
9. Manfield J, Thomas S, Antoniades C, Green A, Fitzgerald J. High resolution photon counting CT permits direct visualisation of directional deep brain stimulation lead segments and markers. Brain Stimulation: Basic, Translational, and Clinical Research in Neuromodulation.
10. Moran C, Sarangmat N, Gerard CS, Barua N, Ashida R, Woolley M, et al. Two hundred twenty-six consecutive deep brain stimulation electrodes placed using an “asleep” technique and the Neuro| MateTM robot for the treatment of movement disorders. Operative Neurosurgery. 2020;19(5):530-38.
11. Li Z, Zhang J-G, Ye Y, Li X. Review on factors affecting targeting accuracy of deep brain stimulation electrode implantation between 2001 and 2015. Stereotactic and functional neurosurgery. 2016;94(6):351-62.
12. McCollough C, Cody D, Edyvean S, Geise R, Gould B, Keat N, et al. The measurement, reporting, and management of radiation dose in CT. Report of AAPM Task Group. 2008;23(23):1-28.
13. Shrimpton PC, Jansen JTM, Harrison JD. Updated estimates of typical effective doses for common CT examinations in the UK following the 2011 national review. The British Journal of Radiology. 2016;89(1057):20150346.
14. Servello D, Zekaj E, Saleh C, Pacchetti C, Porta M. The pros and cons of intraoperative CT scan in evaluation of deep brain stimulation lead implantation: a retrospective study. Surgical neurology international. 2016;7(Suppl 19):S551.
15. Bower KL, Noecker AM, Reich MM, McIntyre CC. Quantifying the Variability Associated with Postoperative Localization of Deep Brain Stimulation Electrodes. Stereotactic and Functional Neurosurgery.1-8.
16. Geevarghese R, O'Gorman Tuura R, Lumsden DE, Samuel M, Ashkan K. Registration accuracy of CT/MRI fusion for localisation of deep brain stimulation electrode position: an imaging study and systematic review. Stereotactic and functional neurosurgery. 2016;94(3):159-63.
17. Neudorfer C, Hunsche S, Hellmich M, El Majdoub F, Maarouf M. Comparative study of robot-assisted versus conventional frame-based deep brain stimulation stereotactic neurosurgery. Stereotactic and functional neurosurgery. 2018;96(5):327-34.
18. Philipp LR, Matias CM, Thalheimer S, Mehta SH, Sharan A, Wu C. Robot-assisted stereotaxy reduces target error: a meta-analysis and meta-regression of 6056 trajectories. Neurosurgery. 2021;88(2):222-33.
19. Cavalcante D, Ghauri MS, Gwinn R. Deep Brain Stimulation Surgery Using a Mobile Intraoperative CT Scanner. Cureus. 2022;14(9).
20. Moran CH, Pietrzyk M, Sarangmat N, Gerard CS, Barua N, Ashida R, et al. Clinical outcome of “asleep” deep brain stimulation for Parkinson disease using robot-assisted delivery and anatomic targeting of the subthalamic nucleus: a series of 152 patients. Neurosurgery. 2021;88(1):165-73.
21. Wall BF. Ionising radiation exposure of the population of the United States: NCRP Report No. 160. Oxford University Press; 2009.

22. Rousseau J, Dreuil S, Bassinet C, Cao S, Elleaume H. Surgivisio® and O-arm® O2 cone beam CT mobile systems for guidance of lumbar spine surgery: comparison of patient radiation dose. Physica Medica. 2021;85:192-99.

Figure Legends

FIGURE 1

Comparison of Ziehm RFD 3D and Medtronic O-arm II imaging Appearances

A. Post-operative DBS Ziehm RFD 3D example imaging- the absence of soft tissue resolution is apparent. B Medtronic O-arm II (3D enhanced mode) example post-DBS image. Here, the rudimentary soft tissue delineation can be appreciated – sufficient for instance to show ventricular configuration.

Figure B image courtesy of Medtronic Inc., reproduced with permission.

FIGURE 2

DBS Workflow Summary

FIGURE 3

Comparison of electrode tip position as assessed on CT-MRI vs 3DXT-MRI fusions

Figure A shows an axial 3DXT image fused to 3T MRI FLAIR with crosshair placed over middle of electrode tip position. In Figure B, the CT is fused with the same MRI sequence. The crosshair is unmoved and electrode position can be seen to appear more lateral (c. 0.5mm which approximates to the 0.41mm average radial fusion variation seen in this series).

Figure C (3DXT to MRI FLAIR fusion) and Figure D (CT to MRI FLAIR fusion) demonstrate the same again, but here the discrepancy is more marked with the electrode on CT appearing anterior and lateral to its position on 3DXT with radial variation c. 1.1mm (the maximum observed in this series).

Evaluation of 3D C-arm fluoroscopy versus diagnostic CT for Deep Brain Stimulation stereotactic registration and post-operative lead localisation

Running Title: 3D fluoroscopy versus CT for DBS registration and lead localisation

James Manfield[1*]
Sean Martin[1]
Alexander L Green[1 2]
James J Fitzgerald [1 2]

[1]Oxford Functional Neurosurgery, John Radcliffe Hospital, Headley Way, Headington, Oxford, OX3 9DU UK
[2]Nuffield Department of Surgical Sciences, University of Oxford, Oxford, UK

*Denotes corresponding author jmanfield@nhs.net

Keywords: DBS imaging; 3D fluoroscopy; robot assisted DBS

Abstract

Introduction

DBS efficacy depends on accuracy. CT-MRI fusion is established for both stereotactic registration and electrode placement verification. The desire to streamline DBS workflows, reduce operative time and minimize patient transfers has increased interest in portable imaging modalities such as the Medtronic O-arm® and mobile CT. However, these remain expensive and bulky. 3D C-arm fluoroscopy (3DXT) units are a smaller and less costly alternative, albeit incompatible with traditional frame-based localisation and without useful soft tissue resolution.
We aimed to compare fusion of 3DXT and CT with pre-operative MRI to evaluate if 3DXT-MRI fusion alone is sufficient for accurate registration and reliable targeting verification. We further assess DBS targeting accuracy using a 3DXT workflow and compare radiation dosimetry between modalities.

Methods

Patients underwent robot-assisted DBS implantation using a workflow incorporating 3DXT which we describe. Two intra-operative 3DXT spins were performed for registration and accuracy verification followed by conventional CT post-operatively.
Post-operative 3DXT and CT images were independently fused to the same pre-operative MRI sequence and co-ordinates generated for comparison.
Registration accuracy was compared to 15 consecutive controls who underwent CT based registration. Radial targeting accuracy was calculated, and radiation dosimetry recorded.

Results

Data were obtained from 29 leads in 15 consecutive patients. 3DXT registration accuracy was significantly superior to CT with mean error 0.22 ±0.03mm ($p<0.0001$).
Mean Euclidean electrode tip position variation for CT to MRI versus 3DXT to MRI fusion was 0.62 ±0.40mm (range 0.0mm – 1.7mm). In comparison, direct CT to 3DXT fusion showed electrode tip Euclidean variance of 0.23 ±0.09mm.
Mean radial targeting accuracy assessed on 3DXT was 0.97 ±0.54mm vs 1.15 ± 0.55mm on CT with differences insignificant ($p = 0.30$).
Mean patient radiation doses were around 80% lower with 3DXT vs CT ($p<0.0001$).

Discussion

Mobile 3D C-arm fluoroscopy can be safely incorporated into DBS workflows for both registration and lead verification. For registration, the limited field of view requires the use of frameless transient fiducials and is highly accurate. For lead position verification based on MRI co-registration, we estimate there is around a 0.4mm discrepancy between lead position seen on 3DXT vs CT when corrected for brain-shift. This is similar to that described in O-arm® or mobile CT series. For units where logistical or financial considerations preclude the acquisition of a cone beam CT or mobile CT scanner, our data support portable 3D C-arm fluoroscopy as an acceptable alternative with significantly lower radiation exposure.

Introduction

DBS efficacy relies on accurate lead targeting[1]. Whilst stereotactic MRI has been regarded by some as the gold standard imaging modality[2], CT-MRI co-registration is an established method for both stereotactic registration and lead placement verification[3]. Fusion inevitably introduces some error, but numerous studies have now quantified this as acceptably small for clinical use[4]. Mobile CT scanners are costly and not yet widely available, so whilst far quicker than MRI, obtaining a CT still typically entails a trip from the operating room. This needs to be repeated twice if used for both stereotactic registration and target confirmation. The desire to streamline DBS workflows, reduce operative time and minimize patient transfers has led to increasing interest in mobile imaging modalities. There are now several published reports using the O-arm® (Medtronic Inc.; Minneapolis, USA), a portable cone beam CT (CBCT) device utilised extensively for spinal surgery, establishing it as a viable option for both DBS stereotactic registration and lead position confirmation[5, 6, 4]. The drawbacks of O-arm include its large footprint, which is not compatible with all operating room set-ups, and expense[7]. We have accordingly acquired the smallest second-generation 3D fluoroscopic C-arm (3DXT; Ziehm RFD 3D, Ziehm Imaging, Germany), which is approximately half the current cost of an O-arm and a similar size to a conventional 2D C-arm. The RFD 3D generates the same power as

an O-arm II with a smaller pixel size, giving the two devices similar bony imaging quality. Among the new 3D-fluoroscopy units, the RFD 3D offers the widest compatibility and integrates with most navigation and robotics platforms[7] – including our recently introduced robot-assisted stereotactic DBS workflow. It does however lack the enhanced soft tissue imaging mode of the O-arm, meaning intra-cranial soft tissue delineation is negligible (See Figure 1). Furthermore, the 20cm field of view (effectively half that of the O-arm's) means an entire human cranium cannot typically be captured within the elliptical 3D spin field and precludes conventional frame based stereotactic registration. Registration must therefore be performed via frameless transient fiducials (FTFR), for which accuracy is established[8]. In view of these limitations of 3DXT, and the lack of published reports supporting its use in DBS, we have further obtained at 24 hours post-op a diagnostic CT scan for confirmation of electrode position, exclusion of significant haematoma prior to discharge, and reconstruction of directional lead contacts[9].

We aim to compare fusion of 3DXT and diagnostic CT with pre-operative planning MRI to evaluate if MRI fusion with 3DXT alone is sufficient for both accurate registration and reliable targeting verification. We further assess DBS targeting accuracy using the 3DXT based workflow, and compare radiation dosimetry between the two modalities.

FIGURE 1 (Comparison of Ziehm RFD 3D and Medtronic O-arm II imaging Appearances)

A. Post-operative DBS Ziehm RFD 3D example imaging- the absence of soft tissue resolution is apparent. B Medtronic O-arm II (3D enhanced mode) example post-DBS image. Here, the rudimentary soft tissue delineation can be appreciated – sufficient for instance to show ventricular configuration.

Figure B image courtesy of Medtronic Inc., reproduced with permission.

Methods

DBS Surgical workflow

Patients underwent robot-assisted DBS implantation using an adapted workflow to incorporating 3DXT in lieu of CT. All patients underwent pre-operative 3T MRI sequences on which the surgical

targeting plan was performed. The Parkinson's disease and dystonia cases were all performed under general anaesthesia with direct targeting. Tremor cases utilising VIM as the surgical target were performed under local anaesthesia +/- conscious sedation to enable intra-operative macrostimulation and assessment. In all cases the CRW frame base ring was used as a head-holder attached to a stereotactic robot (Neuromate; Renishaw, UK). Frameless transient fiducial registration was performed in theatre with a geometrical array mounted on the robotic arm (Neurolocate; Renishaw, UK) in conjunction with a mobile 3DXT (RFD 3D, Ziehm Imaging, Germany). Initial AP and lateral 2D radiographs were obtained to confirm alignment and field of view followed by a 3D spin (Settings: Matrix size 512 x 512, slice thickness – 0.39mm, number of slices 512.) The images were exported to the robotic planning station and detected fiducials manually adjusted until a registration accuracy of <0.25mm was obtained. Image fusion was performed between 3DXT and pre-operative MRI and manually checked. In all cases a fine cut 3D T1-weighted gradient echo was used as the base sequence. A test trajectory to a staple placed on the patient's head prior to imaging was also performed to verify accuracy. The DBS leads were then inserted in keeping with previously described robotic assisted surgical techniques e.g. [10]. Following electrode insertion, a second 3DXT scan was obtained and again fused with pre-operative imaging to confirm targeting accuracy. Following assessment as satisfactory, the case was completed via implantable pulse generator insertion and definitive closure of all wounds. All patients underwent a diagnostic CT scan at 24 hours post op using the same CT scanner in all cases (Siemens Naeotom Alpha, Siemens, Germany) employing a standard CT brain protocol with the following parameters: Acquisition 96 x 0.4mm Volume CT dose index: 55.7; Pitch: 0.35; Rotation Time(s) 0.5; Reconstruction Slice Thickness: 0.6mm; Slice Increment: 0.4mm; Reconstruction Kernel: HR44; Quantum Iterative Reconstruction (QIR) strength: 3; Matrix size: 512 x 512).

FIGURE 2 (DBS Workflow Summary)

Data assessment and analysis

The post-operative 3DXT and diagnostic CT scans were both independently fused to the same pre-operative 3T T1 weighted MR sequence, on which AC-PC co-ordinates had been defined. A trajectory target point was independently created at the tip of the distal electrode contact visualised on CT and 3DXT respectively and co-ordinates generated. To minimise any confounding variation, the right sided contact was always used in bilateral procedures, unless this electrode had been moved

following the 3DXT check scan, in which case the left sided lead was employed. Consistent sequences with equivalent slice thickness (0.4mm for CT and 0.39mm for 3DXT) and standardised windowing settings were employed in all cases. These were chosen so that the tip of the distal contact was unambiguous on multiplanar imaging. The electrode tip was selected as a clear and readily reproducible landmark.

To quantify the impact of post-operative brain shift (e.g. following resolution of any pneumocephalus) rather than fusion variance per se resulting in electrode position discrepancy, the 3DXT and CTs scans were also fused directly to each other as well and co-ordinates generated in the same fashion.

The Euclidean (comprising x, y and z variation) and radial (comprising x and y only) variance between the two generated co-ordinates was calculated using standard formulae[11, 3]. The Euclidean distance is the square root of the sum of squares of the differences in the x, y, and z directions i.e. $\sqrt{[(\Delta x)^2 + (\Delta y)^2 + (\Delta z)^2]}$ with radial comprising $\sqrt{[(\Delta x)^2 + (\Delta y)^2]}$. Vector components were also considered individually.

Registration accuracy is automatically calculated by the planning software based on comparison of the detected to expected fiducial positions. For comparative purposes, data were also obtained from 15 consecutive control cases who underwent conventional CT based registration with CRW frame localiser fiducial box. These cases were performed immediately prior to the introduction for 3DXT and FTFRs and so temporally adjacent. The same planning software was employed in all cases (Renishaw, UK).

Radial targeting accuracy was calculated based on the measured distance between the observed and planned target (typically set at the middle of the first directional contact) as opposed to the electrode tip. All fusion and targeting accuracy assessments were performed manually by the same author to further ensure methodological consistency and minimise variation.

Finally, radiation dosimetry from both scans were noted from contemporaneous documentation.

Results

Patient characteristics

Data were obtained from 29 leads in 15 consecutive patients. All but 1 underwent bilateral DBS insertion involving intra-operative 3DXT and post-operative CT. Patient details are summarised in Table 1.

TABLE 1 (3DXT Patient Characteristics)

Registration Accuracy

For registration with 3DXT plus frameless transient fiducials (FTR), mean registration error was 0.22 ±0.03 mm. For the 15 patient control group with CRW fiducial localiser box CT-based registration, mean error was 0.35 ±0.05 mm. Differences were statistically significant (t test $p<0.0001$) favouring 3DXT.

Demographics between the two groups were very similar with the CT control group having the same sex mix (male:female 6:9) and mean age 63 ± 8.1.

Fusion Variation Assessment

Mean electrode tip position Euclidean variation measured between CT to MRI and 3DXT to MRI fusion was 0.62 ±0.40 mm with range 0.0mm – 1.7mm. Mean radial fusion variance was 0.41mm ± 0.26 mm with range 0.0 mm – 1.1mm.

Mean absolute variation in tip co-ordinates as assessed on 3DXT vs CT to MRI fusion were x 0.22mm (range 0-0.6mm), y 0.28mm (range 0-0.9mm) and z 0.4mm (range 0-1.3mm)

In comparison, direct CT to 3DXT fusion showed electrode tip Euclidean variance of 0.23 ±0.09 mm and radial variance of 0.18mm ±0.08 mm.

Vector components:

Compared with CT-MRI fusion, tip co-ordinates as assessed via 3DXT-MRI fusion were a mean (range) of:

0.007 mm (-0.6 to + 0.4) **right**

0.15 mm (-1 to + 0.4) **posterior**

0.06 mm (-0.9 to +1.3) **superior**

FIGURE 3 (Comparison of electrode tip position as assessed on CT-MRI vs 3DXT-MRI fusions)
Figure A shows an axial 3DXT image fused to 3T MRI FLAIR with crosshair placed over middle of electrode tip position. In Figure B, the CT is fused with the same MRI sequence. The crosshair is unmoved and electrode position can be seen to appear more lateral (c. 0.5mm which approximates to the 0.41mm average radial fusion variation seen in this series).
Figure C (3DXT to MRI FLAIR fusion) and Figure D (CT to MRI FLAIR fusion) demonstrate the same again, but here the discrepancy is more marked with the electrode on CT appearing anterior and lateral to its position on 3DXT with radial variation c. 1.1mm (the maximum observed in this series).

Targeting Accuracy Assessment

Absolute X and Y deviation at planned target as measured on CT-MRI fusion were x mean 0.62mm (SD 0.62mm, range 0-1.47mm) and y 0.31mm (SD 0.54mm, range 0.15-2.1mm). Mean radial error was 1.15mm (SD 0.55mm range 0.3-2.12mm).
Assessed on 3DXT-MRI fusion, absolute x and y deviation were x mean 0.66mm (SD 0.38mm, range 0 -1.24mm) and y mean 0.63mm (SD 0.50mm range 0-1.77mm). Mean radial error was 0.97mm (SD 0.54mm, range 0.26-2.14mm). Assessment differences between the two modalities were not significant (t-test p =0.30).

TABLE 2 (Targeting Accuracy Comparison)

Radiation Dosimetry

Mean CT radiation dose was 942(±54) mGycm. Data were normally distributed (Shapiro-Wilk P = 0.15). This equates to an approximate effective dose of 1.89 mSv [12, 13].

Mean 3DXT radiation doses was 270.1(±74.3) cGycm^2, with all patients receiving two 3D spins. Data were also normally distributed (P = 0.50). Mean approximate absorbed dose was 0.35 mSv (SD 0.10, range 0.21-0.50 mSv). These were significantly less than CT absorbed doses (t test p<0.0001).

Discussion

We have evaluated intra-operative 3DXT use via a 3D C-arm for 29 DBS lead insertions in 15 patients. The mean registration error with 3DXT plus FTFR of 0.22 ±0.03 mm represented a significant improvement compared to our prior CT and frame-based technique. The absolute improvement value of mean 0.13mm is of doubtful clinical significance in isolation but of course contributes to the cumulative error.

Regarding electrode tip localisation, there was a 0.62 ±0.40 mm discrepancy between CT and 3DXT MRI fusion assessment. Part of this variance can be explained by the 24-hour time interval between the scans with re-accumulation of CSF etc. We estimate this effect to explain an average variance of 0.23 ±0.09 mm based on fusing the 3DXT to CT modalities together directly. Such a bone to bone 3DXT to CT fusion has been shown to be highly accurate[14] with minimal error. This leaves a net residual variation of under 0.4mm which may fall within the limitations of human measurement error - other authors for instance have estimated this effect to be around 0.62- 0.7mm[5, 6].

The results should be interpreted in the context that CT to MRI fusion, whilst widely established, remains an intrinsically imperfect process and indeed identical CT and MRI image pairs can produce differing electrode locations, with a median variance of 0.57mm (0.49-0.76mm) noted in one recent study[15], depending on the particular co-registration approach utilised. The software platform used here has been suggested to be amongst the most accurate CT/MRI co-registration algorithms[16] and found to have a geometric fusion error of 0.72 ± 0.08mm[16]. Evaluation of image co-registration typically assumes there is a single ideal solution where the two scans are effectively identical. This may not be entirely true, for instance application of the stereotactic frame adds artifact and distorts scalp outline in addition to the potential geometric distortion of MRI data -particularly with increasing field strength.

These results are comparable to studies evaluating CBCT e.g. O-arm vs CT to MRI co-registration which have for instance found a mean Euclidean difference of 0.886 ±0.190 mm[4]. The interpretation that C-arm based 3DXT is an acceptable alternative to CBCT or CT based techniques is also supported by our overall targeting accuracy results, as assessed on postoperative CT. These subsume both the 3DXT registration scan and the 3DXT post operative check scan on review of

which the decision to accept the final lead position was made. In line with other authors' approach e.g.[17], we have assessed radial accuracy only here as we have found most depth (z coordinate) inaccuracies to be attributable to operator electrode fixation, and easily remediable following the intra-op check scan. The post operative CT imaging therefore reflects any z corrections made following the 3DXT check scan. Radial accuracy is furthermore the most clinically relevant measurement as it directly impacts stimulation efficacy and unwanted effects. Our CT assessed radial accuracy of 1.15 ±0.55 mm was not significantly different from the 0.97 ±0.54 mm as measured on the intra-op 3DXT check scan, and compares acceptably to other published DBS accuracy results[18]. There were no cases where the difference in apparent lead position between the 3DXT and subsequent CT was sufficient to warrant electrode revision.

On a practical note, the 20cm 3DXT 3D FOV means that some of the cranium is typically truncated for the 3D spin. It is suggested that as much of the skull base as possible should be included for an optimum fusion[4]. The outlier case in this series demonstrated a Euclidean fusion discrepancy of 1.7mm (and radial 1.1mm- see Figure 1). We speculate this was caused by mild movement artifact on the MRI scan leading to some peripheral image distortion. With no soft tissue resolution, the 3DXT to MRI fusion relies on fewer data (entirely bony anatomy) and it is thus plausible that it would be subject to greater influence by such image distortion.

Post-operative MRI has its own well known limitations including the size of the electrode related signal void meaning for instance a 1.3mm DBS electrode typically appears to be 2-4mm in diameter[1, 16]. Thus, regardless of the imaging modality employed, some uncertainty surrounding the exact lead position at present remains. Furthermore, due to the aforementioned limited field of view, it is not possible to perform stereotactic imaging with 3DXT. Without stereotactic imaging to generate independent co-ordinates, we cannot conclude from these data which fusion approach (3DXT vs CT) most accurately represents the true position of the electrode. Our conclusions are thus limited to quantifying the variation between the modalities, but support the premise that 3DXT is an acceptable CT or CBCT alternative. There may however be scope for further improvement in 3DXT-MRI fusion. For instance one recent study evaluating a mobile CT scanner (Brainlab Airo) found only a 0.36(±0.54)mm fusion variation between that and conventional CT[19]. Other authors have also described modified 3DXT workflows with for example the addition of IV contrast and region of interest fusion to improve fusion accuracy[20]. Future studies should attempt to quantify the impact of such additional measures to improve 3DXT-MRI fusion accuracy.

Mean patient radiation dose from the two 3DXT spins comprised around 19% of our diagnostic CT doses, and compare favourably to CBCT doses reported in the literature which are typically between 50-100% of conventional CT imaging doses[6, 7, 4]. However, a direct comparison of patient

radiation exposures delivered by CT or CBCT and 3DXT is not possible, as dosimetry is expressed in dose-area product (DAP; mGy.cm.) for 3DXT. and in dose-length product (DLP; mGy.cm) for CBCT and CT. Application of the effective dose (ED) as employed here facilitates estimated comparison of radiation doses from differing modalities by applying appropriate conversion factors to DLP or DAP[21, 22].

Conclusions

Mobile 3D C-arm fluoroscopy can be safely incorporated into DBS workflows for both registration and lead verification purposes. For registration, the limited field of view requires the use of frameless transient fiducials and is highly accurate. For lead position verification based on MRI co-registration, we estimate there is around a net 0.4mm discrepancy between lead position seen on 3DXT vs diagnostic CT when corrected for brain-shift. This is a similar order of magnitude to that described with the well-studied O-arm® and mobile CT scanners. Effective radiation doses for two 3DXT spins were around 20% of conventional CT. For neurosurgical units where logistical or financial considerations preclude the acquisition of a cone beam CT or mobile CT scanner, our data support portable 3D C-arm fluoroscopy as an acceptable alternative.

Statement of Ethics

The study is a service evaluation via retrospective case series review containing no identifiable patient data, for which formal ethical approval was not required (see http://www.hra-decisiontools.org.uk/ethics/ which contains an algorithm to determine what studies require ethical approval in the UK). The 3D C-arm utilised is an approved CE-marked medical device which has neither been modified nor is being used outside of its intended purpose. All patients supplied written informed consent to undergo robot-assisted DBS surgery comprising 3DXT intra-operative and post-operative imaging and for the use of anonymised data for study participation.

Conflict of Interest Statement

The authors have no conflicts of interest to declare.

Funding Sources

This study was not supported by any sponsor or funder.

Author Contributions

JM co-conceived the study, collected data and drafted the manuscript. SM collected data and co-edited the manuscript. JM and JJF analysed data with important intellectual input from AG. All authors critically revised the manuscript.

Data Availability Statement

The data that support the findings of this study are not publicly available due to patient confidentiality but are available from the corresponding author [JM] [jmanfield@nhs.net] subject to necessary anonymisation upon reasonable request.

References

1. Mirzadeh Z, Chapple K, Lambert M, Dhall R, Ponce FA. Validation of CT-MRI fusion for intraoperative assessment of stereotactic accuracy in DBS surgery. Movement Disorders. 2014;29(14):1788-95.
2. Bot M, Van Den Munckhof P, Bakay R, Stebbins G, Verhagen Metman L. Accuracy of intraoperative computed tomography during deep brain stimulation procedures: comparison with postoperative magnetic resonance imaging. Stereotactic and Functional Neurosurgery. 2017;95(3):183-88.
3. Furlanetti L, Hasegawa H, Oviedova A, Raslan A, Samuel M, Selway R, et al. O-arm stereotactic imaging in deep brain stimulation surgery workflow: a utility and cost-effectiveness analysis. Stereotactic and Functional Neurosurgery. 2021;99(2):93-106.
4. Peng T, Kramer DR, Lee MB, Barbaro MF, Ding L, Liu CY, et al. Comparison of intraoperative 3-dimensional fluoroscopy with standard computed tomography for stereotactic frame registration. Operative Neurosurgery. 2020;18(6):698.
5. Holloway K, Docef A. A quantitative assessment of the accuracy and reliability of O-arm images for deep brain stimulation surgery. Operative Neurosurgery. 2013;72:ons 47-ons 57.
6. Carlson JD, McLeod KE, McLeod PS, Mark JB. Stereotactic accuracy and surgical utility of the O-arm in deep brain stimulation surgery. Operative Neurosurgery. 2017;13(1):96-107.
7. Malham GM, Wells-Quinn T. What should my hospital buy next?—guidelines for the acquisition and application of imaging, navigation, and robotics for spine surgery. Journal of Spine Surgery. 2019;5(1):155.

8. Hines K, Matias CM, Leibold A, Sharan A, Wu C. Accuracy and efficiency using frameless transient fiducial registration in stereoelectroencephalography and deep brain stimulation. Journal of Neurosurgery. 2022;1(aop):1-7.
9. Manfield J, Thomas S, Antoniades C, Green A, Fitzgerald J. High resolution photon counting CT permits direct visualisation of directional deep brain stimulation lead segments and markers. Brain Stimulation: Basic, Translational, and Clinical Research in Neuromodulation.
10. Moran C, Sarangmat N, Gerard CS, Barua N, Ashida R, Woolley M, et al. Two hundred twenty-six consecutive deep brain stimulation electrodes placed using an “asleep” technique and the Neuro| MateTM robot for the treatment of movement disorders. Operative Neurosurgery. 2020;19(5):530-38.
11. Li Z, Zhang J-G, Ye Y, Li X. Review on factors affecting targeting accuracy of deep brain stimulation electrode implantation between 2001 and 2015. Stereotactic and functional neurosurgery. 2016;94(6):351-62.
12. McCollough C, Cody D, Edyvean S, Geise R, Gould B, Keat N, et al. The measurement, reporting, and management of radiation dose in CT. Report of AAPM Task Group. 2008;23(23):1-28.
13. Shrimpton PC, Jansen JTM, Harrison JD. Updated estimates of typical effective doses for common CT examinations in the UK following the 2011 national review. The British Journal of Radiology. 2016;89(1057):20150346.
14. Servello D, Zekaj E, Saleh C, Pacchetti C, Porta M. The pros and cons of intraoperative CT scan in evaluation of deep brain stimulation lead implantation: a retrospective study. Surgical neurology international. 2016;7(Suppl 19):S551.
15. Bower KL, Noecker AM, Reich MM, McIntyre CC. Quantifying the Variability Associated with Postoperative Localization of Deep Brain Stimulation Electrodes. Stereotactic and Functional Neurosurgery.1-8.
16. Geevarghese R, O'Gorman Tuura R, Lumsden DE, Samuel M, Ashkan K. Registration accuracy of CT/MRI fusion for localisation of deep brain stimulation electrode position: an imaging study and systematic review. Stereotactic and functional neurosurgery. 2016;94(3):159-63.
17. Neudorfer C, Hunsche S, Hellmich M, El Majdoub F, Maarouf M. Comparative study of robot-assisted versus conventional frame-based deep brain stimulation stereotactic neurosurgery. Stereotactic and functional neurosurgery. 2018;96(5):327-34.
18. Philipp LR, Matias CM, Thalheimer S, Mehta SH, Sharan A, Wu C. Robot-assisted stereotaxy reduces target error: a meta-analysis and meta-regression of 6056 trajectories. Neurosurgery. 2021;88(2):222-33.
19. Cavalcante D, Ghauri MS, Gwinn R. Deep Brain Stimulation Surgery Using a Mobile Intraoperative CT Scanner. Cureus. 2022;14(9).
20. Moran CH, Pietrzyk M, Sarangmat N, Gerard CS, Barua N, Ashida R, et al. Clinical outcome of “asleep” deep brain stimulation for Parkinson disease using robot-assisted delivery and anatomic targeting of the subthalamic nucleus: a series of 152 patients. Neurosurgery. 2021;88(1):165-73.
21. Wall BF. Ionising radiation exposure of the population of the United States: NCRP Report No. 160. Oxford University Press; 2009.

22. Rousseau J, Dreuil S, Bassinet C, Cao S, Elleaume H. Surgivisio® and O-arm® O2 cone beam CT mobile systems for guidance of lumbar spine surgery: comparison of patient radiation dose. Physica Medica. 2021;85:192-99.

Figure Legends

FIGURE 1

Comparison of Ziehm RFD 3D and Medtronic O-arm II imaging Appearances

A. Post-operative DBS Ziehm RFD 3D example imaging- the absence of soft tissue resolution is apparent. B Medtronic O-arm II (3D enhanced mode) example post-DBS image. Here, the rudimentary soft tissue delineation can be appreciated – sufficient for instance to show ventricular configuration.

Figure B image courtesy of Medtronic Inc., reproduced with permission.

FIGURE 2

DBS Workflow Summary

FIGURE 3

Comparison of electrode tip position as assessed on CT-MRI vs 3DXT-MRI fusions

Figure A shows an axial 3DXT image fused to 3T MRI FLAIR with crosshair placed over middle of electrode tip position. In Figure B, the CT is fused with the same MRI sequence. The crosshair is unmoved and electrode position can be seen to appear more lateral (c. 0.5mm which approximates to the 0.41mm average radial fusion variation seen in this series).

Figure C (3DXT to MRI FLAIR fusion) and Figure D (CT to MRI FLAIR fusion) demonstrate the same again, but here the discrepancy is more marked with the electrode on CT appearing anterior and lateral to its position on 3DXT with radial variation c. 1.1mm (the maximum observed in this series).

TABLE 1 (3DXT Patient Characteristics)

Number of patients and DBS leads	15 patients with 29 leads in total
Age (mean ± SD)	64 ± 8.3
Sex (Male:Female)	6:9
Diagnoses:	
Parkinson's disease (n,%)	10, 67%
Essential tremor (n,%)	4, 27%
Dystonia (n,%)	1, 6.7%
Anatomical Target:	
STN (n,%)	10, 67%
VIM (n,%)	4, 27%
GPi (n,%)	1, 6.7%

TABLE 2 (Targeting Accuracy Comparison)

Mean absolute differences ±SD (mm) (95% CI) between planned and actual lead trajectories at x and y co-ordinates as assessed with either CT or 3DXT:

Co-ordinate	**CT**	**3DXT**	**Significance (p value)**
x	0.62 ± 0.51mm	0.66 ± 0.38mm	P = 0.81
y	0.83 ± 0.54mm	0.63 ± 0.50mm	P = 0.22
Radial distance	1.15 ± 0.55mm	0.97 ± 0.54mm	P = 0.30

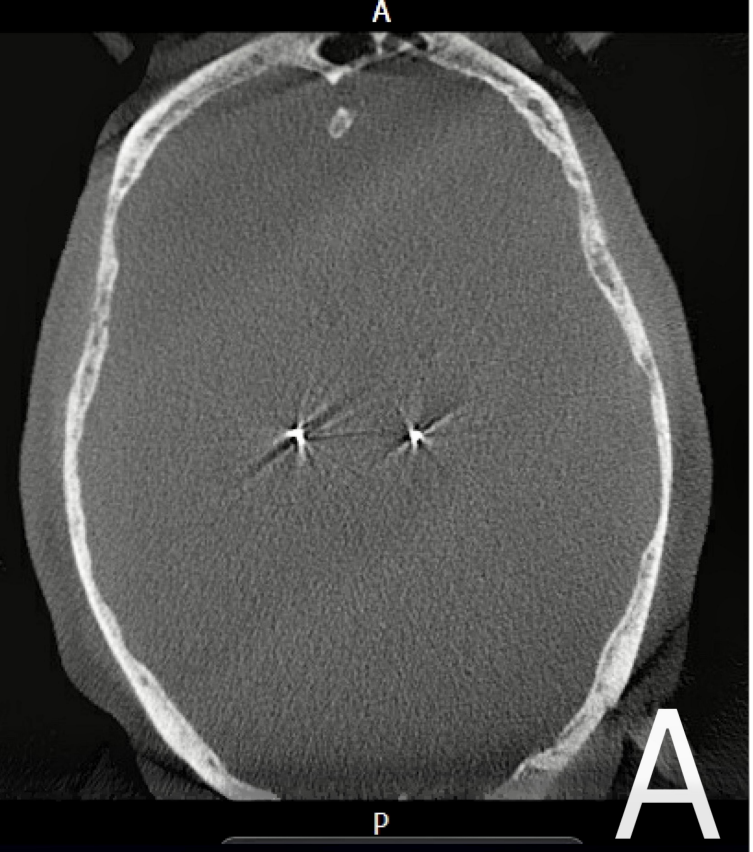
A
P
A

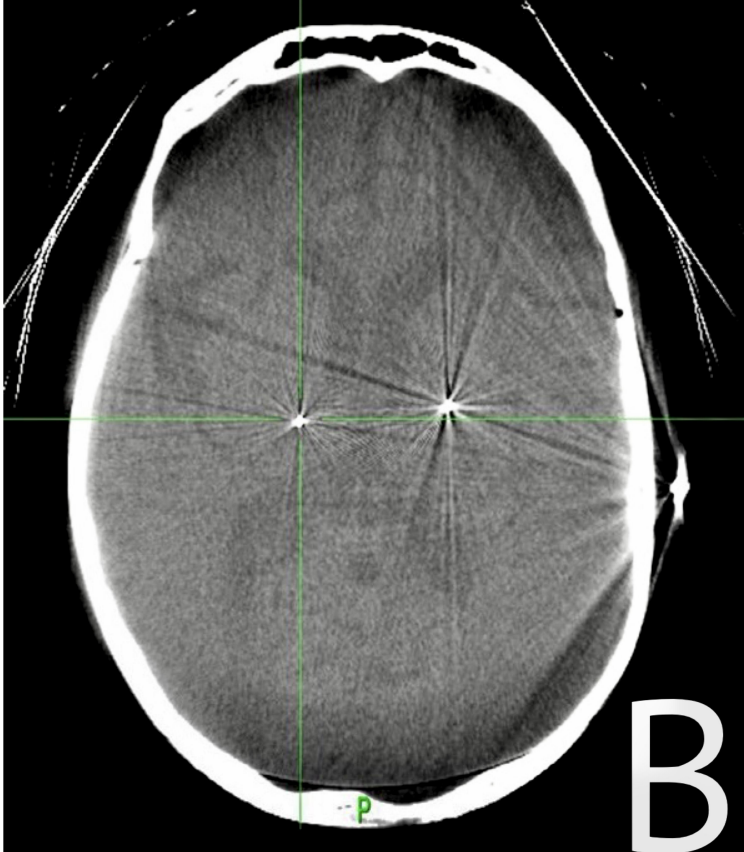
P
B

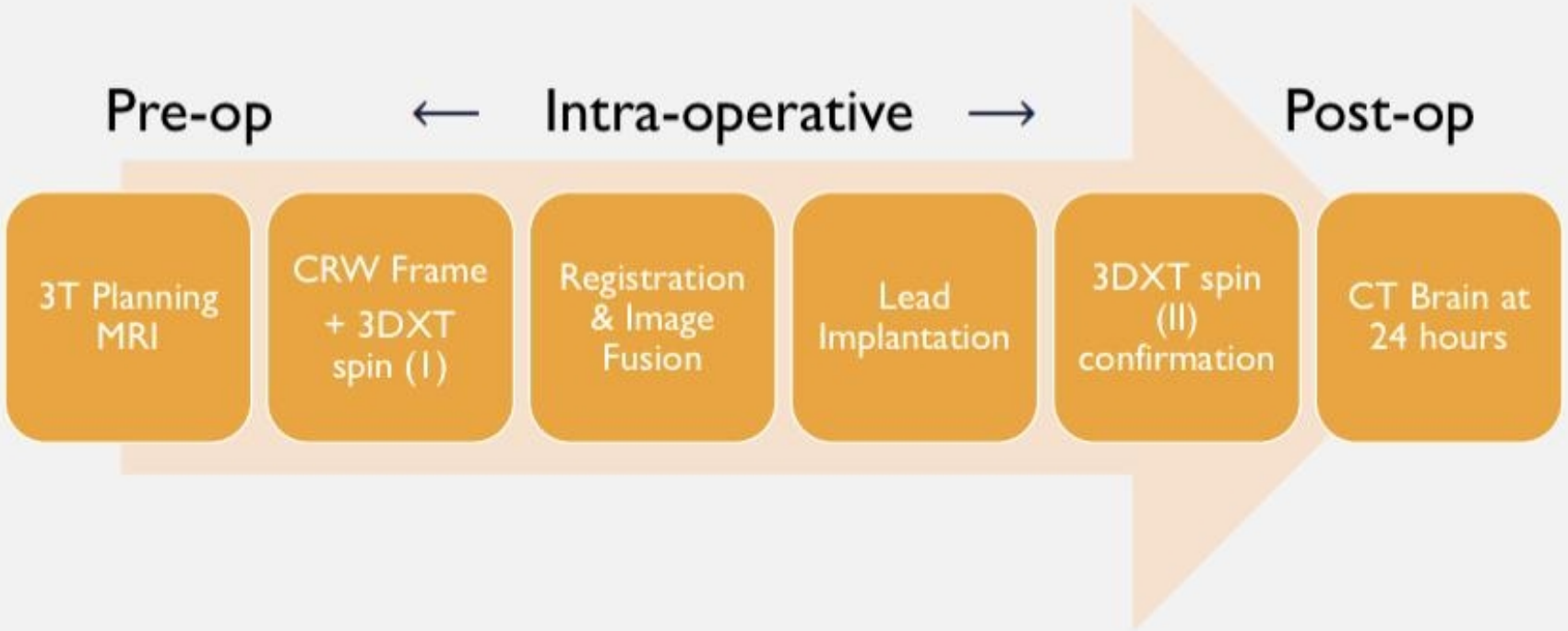
Pre-op
Intra-operative
Post-op
3T Planning MRI
CRW Frame + 3DXT spin (I)
Registration & Image Fusion
Lead Implantation
3DXT spin (II) confirmation
CT Brain at 24 hours

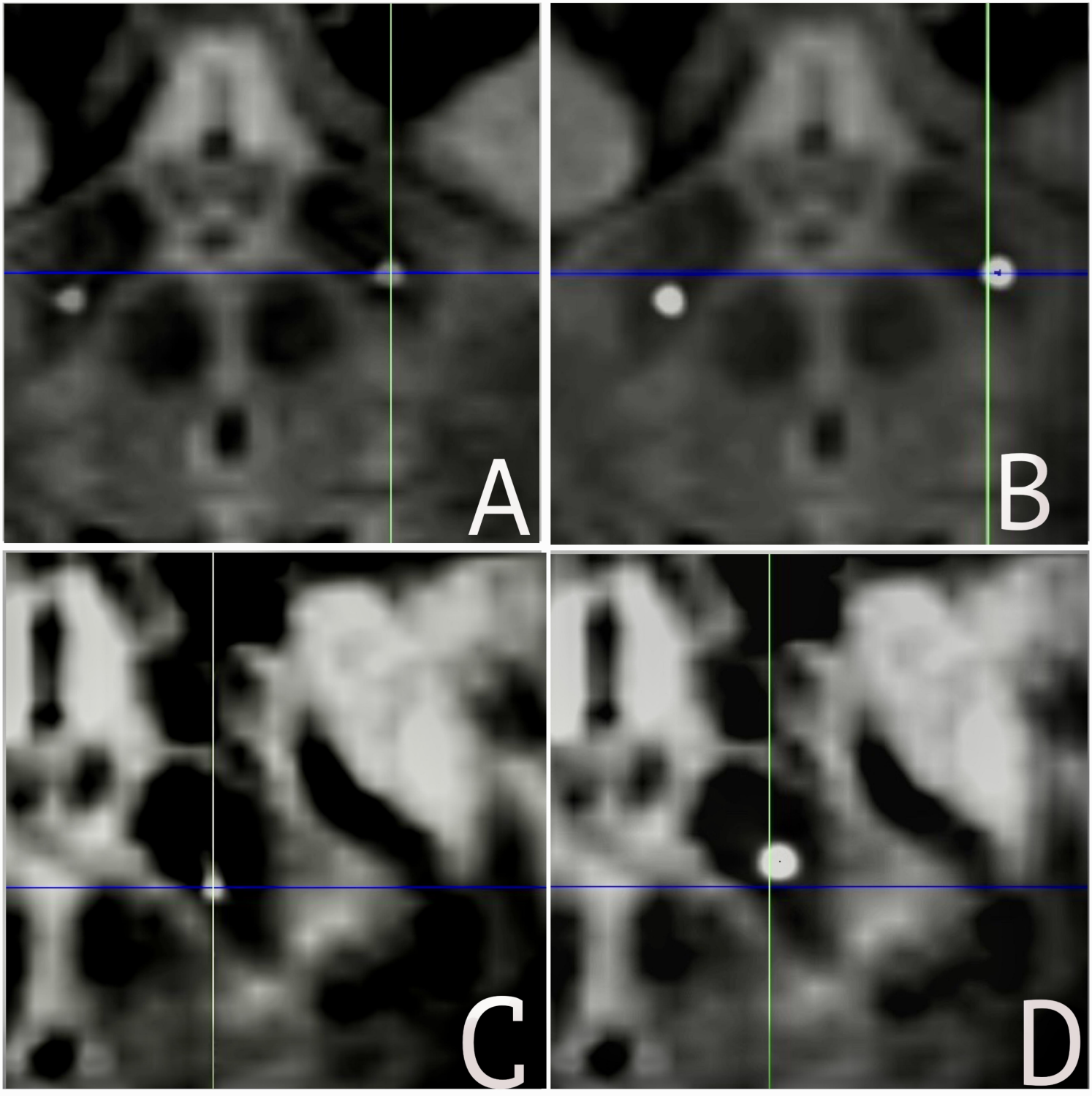
A
B
C
D